HF WAVEGUIDE LASER STUDY

Final Report

by
A. Stein

AIL REPORT NO. C416-2
April 1977

Prepared under Contract N00014-76-C-0397
Office of Naval Research
Washington, D.C.

Sponsored by
ADVANCED RESEARCH PROJECTS AGENCY
ARPA Order No. 1806, Amendment No. 25

AIL a division of CUTLER-HAMMER
DEER PARK, LONG ISLAND, NEW YORK 11729

HF WAVEGUIDE LASER STUDY

Final Report, 8 Dec 75 – 7 Dec 76,

by
A. Stein

Apr 77

AIL REPORT NO. C416-2
April 1977

57 p.

Prepared under Contract N00014-76-C-0397, ARPA Order 1806
Office of Naval Research
Washington, D.C.

Sponsored by
ADVANCED RESEARCH PROJECTS AGENCY
ARPA Order No. 1806, Amendment No. 25

AIL a division of CUTLER-HAMMER
DEER PARK, LONG ISLAND, NEW YORK 11729

404967

CONTRACT NO.:	N00014-76-C-0397
ARPA ORDER NO.:	1806, Amend. 25
PROGRAM CODE:	6E20
NAME OF CONTRACTOR:	AIL, a division of Cutler-Hammer
EFFECTIVE DATE OF CONTRACT:	Dec. 8, 1975
CONTRACT EXPIRATION DATE:	Dec. 7, 1976
CONTRACT AMOUNT:	$99,392
PRINCIPAL INVESTIGATOR:	Dr. A. Stein (516)-595-4405
SCIENTIFIC OFFICER:	Office of Naval Research 800 N. Quincy Street Arlington, Virginia 22217 Attn: Code 421, Dr. M.B. White

DISCLAIMER: The views and conclusions contained in this document are those of the author's and should not be interpreted as necessarily representing the official policies, either expressed or implied, of the Advanced Research Projects Agency or the U.S. Government.

ACKNOWLEDGEMENTS

The author would like to acknowledge the expert assistance of AIL staff member Mr. L. Saarikko. This work was carried out in the Infrared and Electro-Optics Department, under B.J. Peyton, Department Head.

SECURITY CLASSIFICATION OF THIS PAGE *(When Data Entered)*

REPORT DOCUMENTATION PAGE

READ INSTRUCTIONS BEFORE COMPLETING FORM

REPORT NUMBER — C416-2	2. GOVT ACCESSION NO.
3. RECIPIENT'S CATALOG NUMBER	
4. TITLE *(and Subtitle)* Waveguide HF Laser	5. TYPE OF REPORT & PERIOD COVERED Final 8 Dec. 1975 - 7 Dec. 1976
6. PERFORMING ORG. REPORT NUMBER	
7. AUTHOR(s) A. Stein	8. CONTRACT OR GRANT NUMBER(s) N00014-76-C-0397
9. PERFORMING ORGANIZATION NAME AND ADDRESS AIL, division of Cutler-Hammer Deer Park, New York 11729	10. PROGRAM ELEMENT, PROJECT, TASK AREA & WORK UNIT NUMBERS
11. CONTROLLING OFFICE NAME AND ADDRESS Office of Naval Research 800 N. Quincy Street Arlington, Virginia 22217	12. REPORT DATE April 1977
	13. NUMBER OF PAGES
14. MONITORING AGENCY NAME & ADDRESS(if different from Controlling Office)	15. SECURITY CLASS. *(of this report)* Unclassified
	15a. DECLASSIFICATION/DOWNGRADING SCHEDULE

16. DISTRIBUTION STATEMENT *(of this Report)*

DISTRIBUTION STATEMENT A
Approved for public release;
Distribution Unlimited

17. DISTRIBUTION STATEMENT *(of the abstract entered in Block 20, if different from Report)*

18. SUPPLEMENTARY NOTES

19. KEY WORDS *(Continue on reverse side if necessary and identify by block number)*

HF laser Waveguide laser

20. ABSTRACT *(Continue on reverse side if necessary and identify by block number)*

The feasibility of a purely electrical excitation mechanism for HF waveguide lasers was investigated whereby HF molecules are heavily diluted in a helium buffer gas and vibrationally excited through inelastic collisions in a discharge confined to a 1 x 1 mm channel of 8 cm length.

over

DD FORM 1 JAN 73 1473 EDITION OF 1 NOV 65 IS OBSOLETE

404 967

SECURITY CLASSIFICATION OF THIS PAGE *(When Data Entered)*

2.0 ABSTRACT (continued)

Among the many HF vibration-rotation transitions there are several candidates for laser action. The relative population of their respective initial and terminal levels was ascertained from the measured intensity of the associated fluorescence. The data indicated inversion for some of the high J-number P-transitions. But since these levels were sparsely populated the resulting gain was extremely small and blanketed by scattering losses.

A peak electron density of $\sim 1 \times 10^{12}$ cm^{-3} was achieved with this simple, self-sustained discharge. It is suggested that further increases in electron density and observable laser action can be attained by adding appropriate preionization to this discharge.

Such a laser would be compact and could in principle be operated in closed-cycle fashion.

A further result of this program is a direct demonstration of delayed H_2 to HF excitation transfer.

TABLE OF CONTENTS

LIST OF ILLUSTRATIONS

1.0 INTRODUCTION

During the past several years the development of HF(DF) lasers has progressed to the point where this technology may now be directed towards pointing and tracking, optical radar, optical communication and general surveillance applications. However the implementation of these applications must await the development of stable, low power HF(DF) laser sources which could be used as master and local oscillators in conjunction with the already existing power amplifiers.

CW chemical HF lasers employ a flowing gas mix to provide vibrational activation of HF via an exothermic chemical reaction between hydrogen and fluoride. Fresh reactants are continuously supplied and the spent gases are exhausted. These systems are not only bulky but the need for safe removal of the poisonous exhaust limits their applications (References 1 and 2).

This program was aimed towards the development of a purely electrical, compact HF waveguide laser which could in principle be operated with a sealed vessel containing HF diluted in a buffer gas. Smaller size and weight, elimination of poisonous exhausts and greater potential frequency and amplitude stability are the attractive features of such a device. The small plasma volume limits the expected average output power to a low value but permits repetitively pulsed excitation up to 10^4-10^5 pps.

Chemical HF lasers presently cannot be pulsed efficiently at such extreme repetition rates. While the HF waveguide laser is ideally suited for this mode of operation, its output could be boosted to a desired higher level by conventional CW chemical laser

amplifiers. Such a combination represents an attractive source for optical pulse-radar applications.

If CW laser action can be achieved, the application of this device as a local oscillator in a coherent receiver would offer distinct advantages over the chemical lasers in size, ease of handling and stability.

The feasibility of purely electrical HF and DF lasers has been previously demonstrated for pulsed excitation using an electron-beam stabilized, transverse discharge in a relatively large active volume (5 cm x 5 cm x 50 cm) (References 3 and 4).

It was recognized that such a system could be operated at high pulse rates and even continuously if the active volume was scaled down transversely to a channel of millimeter diameter or less.

2.0 LASER INVERSION MECHANISM

2.1 He/HF DISCHARGES

To obtain a high rate of excitation collisions one would like the density of both collision partners, electrons and HF molecules, to be as high as possible. But at higher HF concentrations, self-quenching collisions will increase reducing the net pumping rate. There is thus an optimum HF pressure (a few torr) for which the attainable relative population density in the first vibrational level is largest. But a discharge in such a rarefied gas will not yield the required electron densities of 10^{12}-10^{13} cm^{-3} and a buffer gas of higher partial pressure must be added to support a discharge of high current density (Reference 3). During this program helium was used as buffer gas at pressures varying between 150 and 500 torr.

When diatomic molecules are excited to their first vibrational state, v = 1, by collisions with the free plasma electrons, higher vibrational modes are activated through energy transfer in collisions between those excited molecules. This process, crucial to the functioning of CO lasers, is called "ladder climbing", and generates a non-Boltzmann vibrational population distribution which may create total level inversion among neighboring v-states (References 5 and 6). However, for the short discharge pulses investigated here, ladder climbing does not properly develop and only excitation of the first vibrational state HF(1) need be considered. In this case, level inversion can only be partial; i.e., for selected rotational quantum numbers. This kind of inversion is due to a large difference between the rotational and the vibrational temperatures which develop in a He/HF discharge where the vibrational and rotational modes of HF are excited by collisions with the free electrons and relaxation occurs in collisions with other molecules. The reason for this phenomenon is the large difference in the relaxation rates for the rotational and vibrational states (Reference 7).

It can be shown (Appendix A) that the condition for laser gain is given by

$$\frac{2JB}{T_r} \geq \frac{w_e}{T_v} \qquad (1)$$

J = rotational quantum number

B = rotational energy constants of HF = 20.9 cm^{-1}

w_e = vibrational energy constant of HF = 4138.5 cm^{-1}

T_r = rotational temperature for the v = 0 and v = 1 level system

T_v = vibrational temperature associated with the population ratio of the v = 1 and v = 0 states

Total population inversion corresponds to a negative value for T_v which obviously fulfills condition (1).

The choice of He as buffer gas was in part based on its ability to provide rapid cooling of the collisional motion of HF and transfer the thermal energy to the walls of the discharge vessel. The rotational temperature is approximately equal to the kinetic gas temperature ($\approx 300^{\circ}K$) while the vibrational temperature takes on a value somewhere between the gas temperature and the electron temperature.

2.2 $He/H_2/HF$ DISCHARGES

The addition of hydrogen to the He/HF mix provides a second excitation mechanism for the HF(1) state. Here, vibrational energy is transferred from the electron-collision-excited H_2 to the HF molecules and the H_2 acts as an intermediate energy storage medium.

While the partial pressure of HF cannot be increased beyond a few torr because of self-quenching, the pressure of H_2 can be increased to higher values to optimize the transfer of primary energy from the free plasma electrons to the molecular vibrations of interest. Self-quenching of H_2 is negligible and the secondary energy transfer via the following collision reaction,

$$H_2(1) + HF(0) \underset{k^-}{\overset{k^+}{\rightleftarrows}} H_2(0) + HF(1), \qquad (2)$$

is very efficient since reaction (2) dominates all other competing depopulation mechanism for $H_2(1)$ within some limits of H_2 partial pressure (Reference 8).

It can be shown (Appendix B) that the population ratios of excited to ground state levels for H_2 and HF are given by

$$\frac{N_1}{N_0} = \frac{M_1}{M_0} \frac{e^{\Delta E/kT}}{1 + \frac{k_1 N_0}{k^- M_0}} \qquad (3)$$

T = kinetic gas temperature

N_1, N_0 = population densities for HF(1), HF(0), respectively

M_1, M_0 = population densities for $H_2(1)$, $H_2(0)$, respectively

ΔE = difference in vibrational energy constant between hydrogen and hydrogen fluoride $\sim$ 200 cm^{-1} hc

k^- = reaction rate for transfer process = 1.7 10^4 sec^{-1} $torr^{-1}$ (Reference 9)

k_1 = self-quenching rate for HF(1) = 6 10^4 (Reference 10)

Inspecting equation (3) one notes that the term $k_1 N_0 / k^- M_0$ should be as small as possible for efficient excitation transfer. The concentration of H_2 should therefore be several times larger than that of HF. As an example, if $M_0 = 10\ N_0$ it follows from equation (3) that $\frac{N_1}{N_0} \approx 2 \frac{M_1}{M_0}$ and therefore the degree of excitation for HF is twice that for the activating gas.

3.0 LASER DEVICE

3.1 SELF-SUSTAINED DISCHARGE UNIT

The HF waveguide laser employs a transverse discharge geometry where the electrode surfaces are spaced by 1 mm forming two opposing walls of a rectangular channel while the other two walls are filled in by the edges of 1 mm thick sapphire spacers as illustrated in Figure 1. A pulsed glow discharge is struck transversely to the channel while optical propagation proceeds along the channel axis.

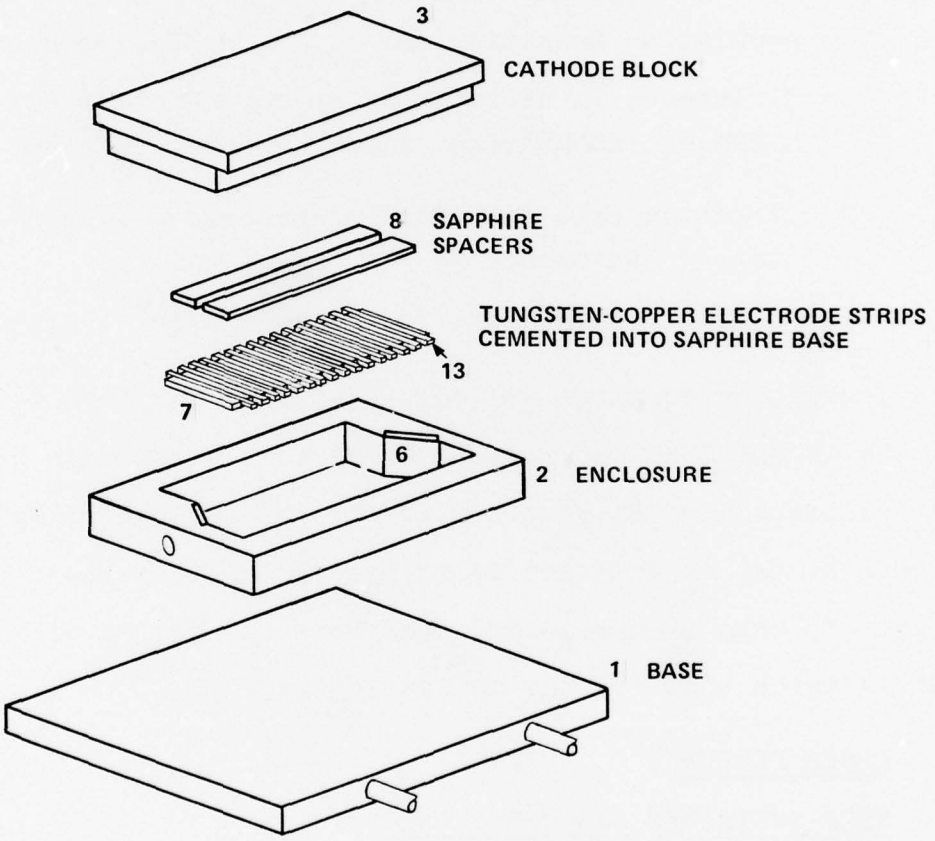

Figure 1. Self-Sustained Discharge Unit - Exploded View.

Such a device was originally developed for pulsed CO_2 lasers operating at atmospheric gas pressures (Reference 11). The main reason for its application to the HF/He discharge is the ability to conduct the high thermal energy of the discharge plasma rapidly to the vessel enclosure because of the capillary geometry. Such a transversely excited HF waveguide unit can be operated at very high pulse repetition rates whereas a larger volume system requires a considerably longer recovery period between pulses to allow the gas to cool to ambient temperatures (References 3 and 4). A further advantage of a transversely excited capillary discharge is the ability to generate a uniform glow discharge and suppress the formation of arcs even at relatively high gas pressures and current densities. (Although the HF waveguide laser was designed for sealed off operation, a gas flow was maintained during these experiments for good turbulent mixing in the plasma to prevent any local temperature build-up, which could serve as a starting point for an arc.) In addition, narrow gap discharges require much lower drive voltages than longitudinal ones. Finally, the required volume flow rate is small easing the problem of handling toxic gases such as HF in a laboratory, and reducing the cost for expensive gases such as DF or D_2.

Since the capillary channel is too narrow to clear a free space Gaussian wave, this liability can be converted into an asset by using polished surfaces such that the channel acts as an optical waveguide for the propagated laser beam. Such a combination of waveguide and capillary discharge principles is a well developed

technique and has led to remarkable success in extending the frequency tuning range and reducing the size of several laser species (References 12 and 13).

The discharge channel assembly as shown in Figure 1 rests on a copper base and is enclosed by a teflon shell. An aluminum block slides into the shell such that its bottom surface contacts the sapphire spacers closing off the channel. Brewster-angled sapphire windows sealed to the teflon shell provide passage for the laser beam. The anode is broken up into an array of 50 metallic strips embedded into a sapphire plate. Individual discharges are formed between each anode element and the foil in TEA laser fashion.

A schematic diagram of the electrical circuitry for the single pulse discharges is shown in Figure 2. The 50 capacitors C_i are charged through the individual resistors R_i from a common supply which is also connected to the cathode. Upon trigger command, a thyratron provides a low impedance path to ground causing the capacitor voltage to appear across the 50 discharge gaps.

A photograph of the laser head is presented in Figure 3. The leads connecting the discharge capacitors to the anode strips are visible as are the charge resistors which are also connected to the anode strips. The gas input and output lines and the cooling water lines are also shown. The thyratron is visible in the background and the two laser reflector assemblies are seen on either side of the discharge unit.

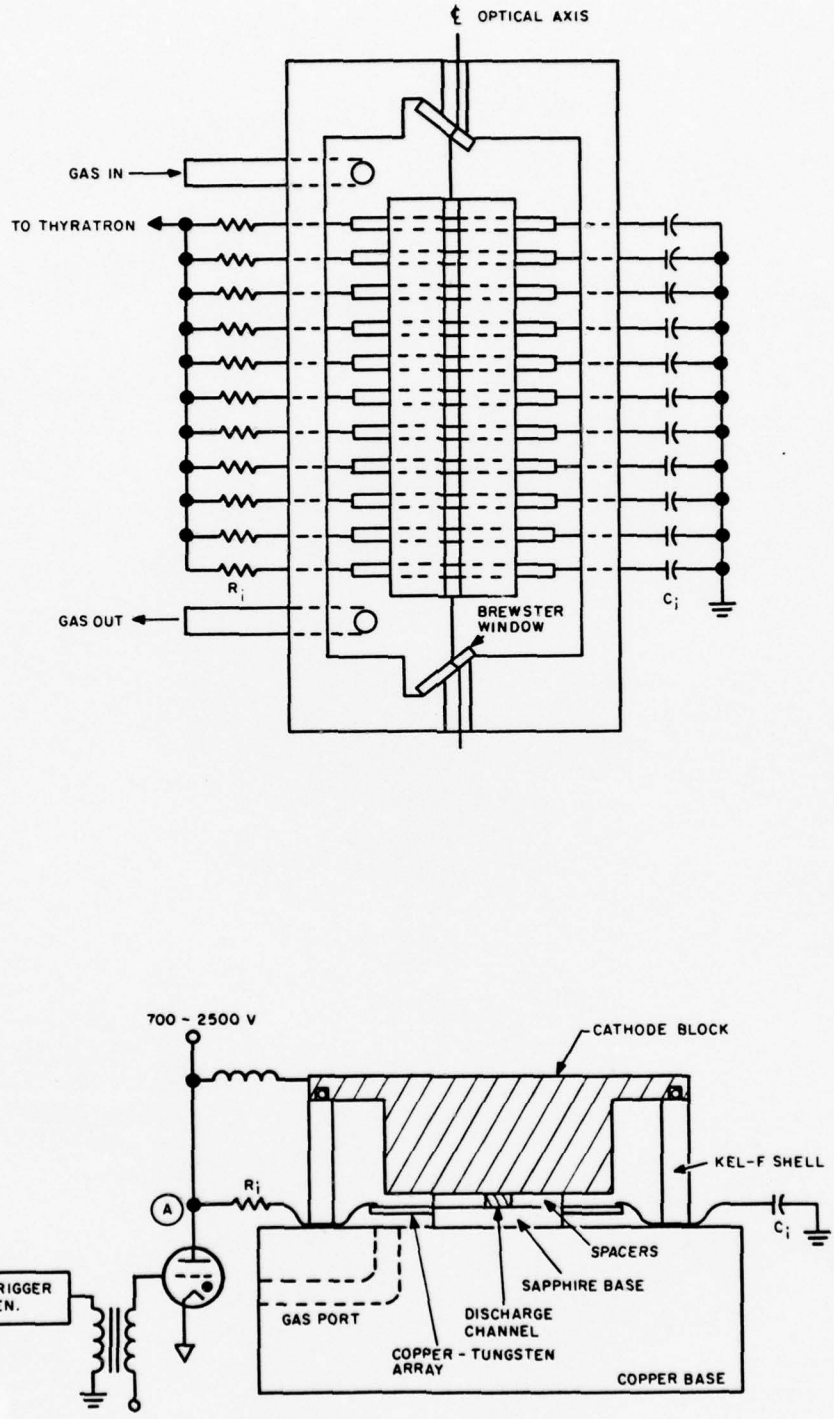

Figure 2. Self-Sustained Discharge Unit with Electrical Circuit.

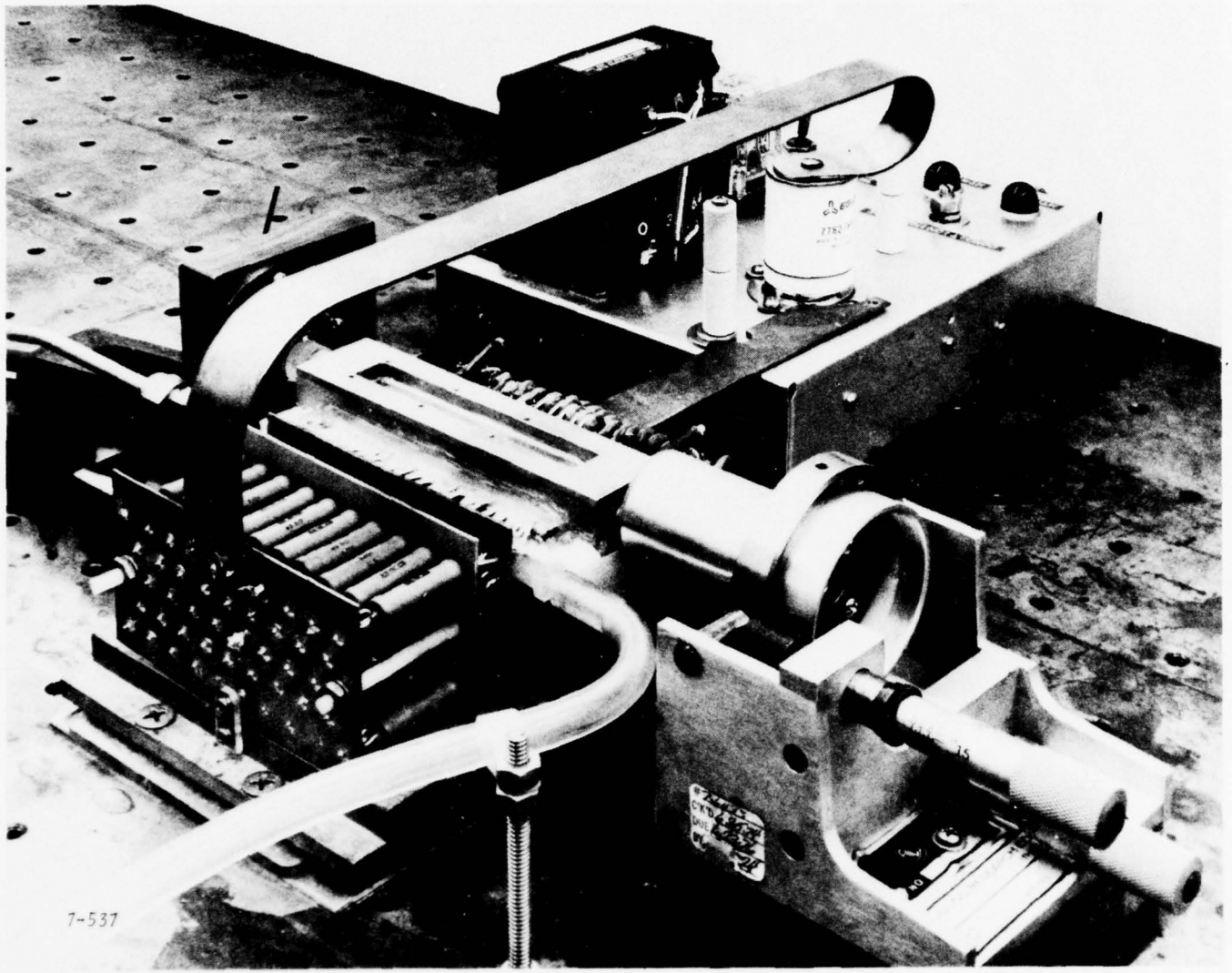

Figure 3. Self-Sustained HF Waveguide Laser

The laser gases are released from pressurized containers and accurately metered into a mixing manifold from which they enter the discharge volume. A mechanical vacuum pump then removes the gases from the laser system. The research grade gases were obtained from Mathieson Co. Hydrogen fluoride was purchased in a small lecture bottle which was chilled to about $10^{\circ}C$, well below the boiling point of HF. The overall experimental setup is shown in Figure 4. The pumps and the gas handling apparatus are in the foreground and the laser head is on the right side of the optical table next to the discharge circuitry. Not shown is the fluorescence measurement equipment which was located on the optical bench during measurements.

3.2 ELECTRON-GUN AUGMENTED DISCHARGE UNIT

The previously reported HF discharge lasers employed electron-beam-stabilized discharges (References 3 and 4) and were a good deal more complex than the ordinary discharge apparatus because of the electron gun. The advantage of this device is that the injected electron beam provides the necessary ionization to replenish the charge carriers lost by recombination. The drift field can be very small under those circumstances, which is more favorable to the excitation of vibrational modes in HF.

In self-sustained discharges on the other hand, the task of charge replenishment rests with the discharge electrons themselves. Here the drift field must be much higher to yield a certain number of energetic electrons capable of ionizing the gas molecules. Therefore, the field necessary to strike a discharge

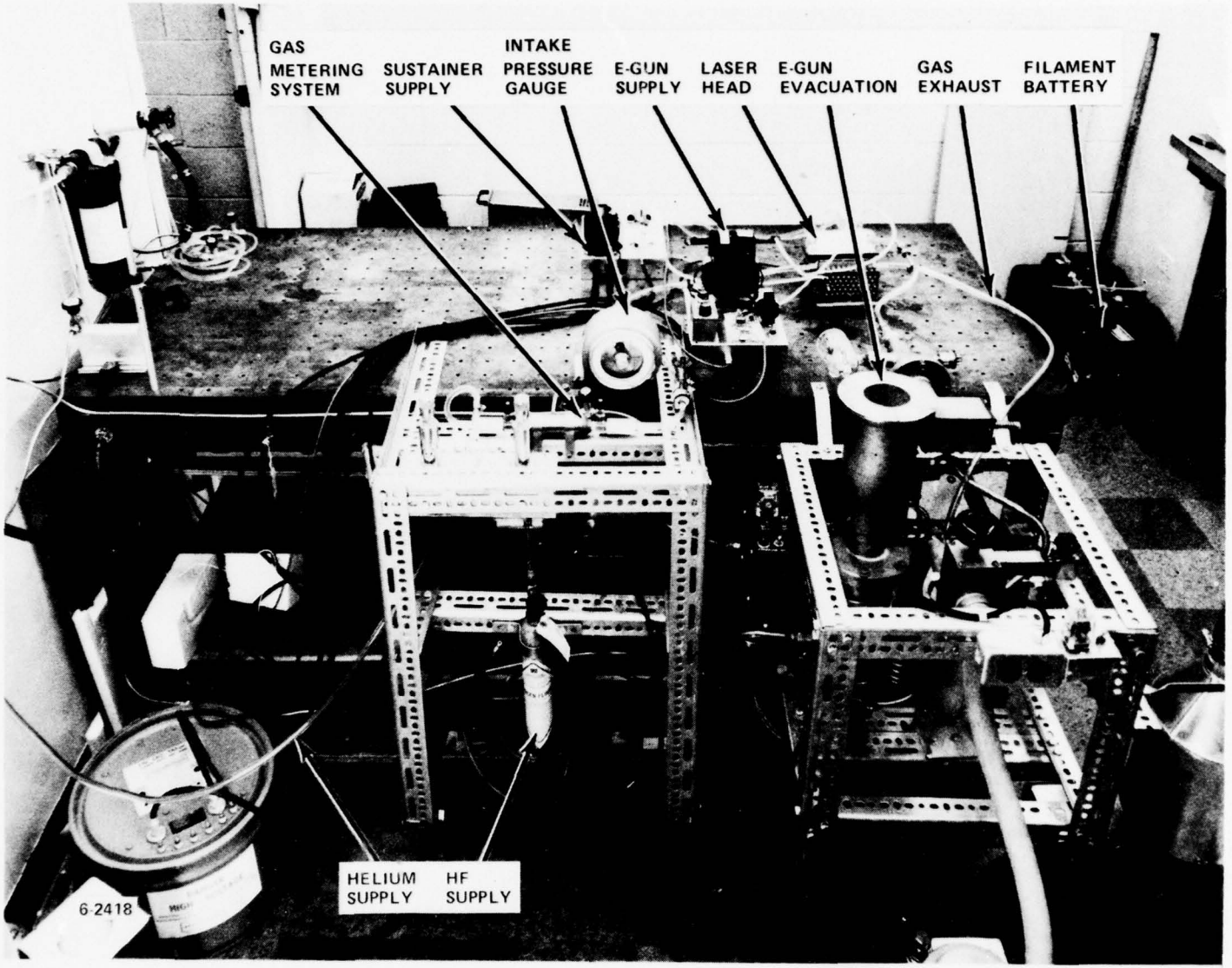

Figure 4. Experimental Setup

is much larger than the field which optimizes vibrational excitation, and the gas heating is accordingly large. Consequently, there is a danger that a CW-glow discharge may degenerate into an arc. The arcing is not necessarily a problem for pulsed discharges as our experimental observations have demonstrated (Section 4).

For the larger part of the contract period, the effort was concentrated on developing an electron-gun-augmented discharge unit.

In order to integrate an electron-gun with the transverse discharge vessel one of the metallic channel walls was constructed from a thin titanium foil serving as the septum between the gas-filled discharge channel and the evacuated electron-gun. The gun consisted of a heated linear filament strung out parallel to the channel. The emitted electrons were accelerated towards the titanium foil, penetrated the foil and then entered the discharge plasma, where they ionized the gas and thus replenished the charge carriers lost to diffusion and recombination. In addition to the E-beam, an electrical dc-potential was applied across the 1 mm channel gap to sustain the discharge: i.e., conduct the secondary electrodes through the gas.

Because of the narrow channel dimensions, the mechanical stress on the foil was very small permitting the use of 0.0001" titanium foil. The advantage of using such a thin foil is that it takes only a relatively low E-gun voltage ($\sim$50 keV) to obtain an electron transmission of $>$ 80 percent (see Appendix C).

However, it was found during the course of these experiments that extremely thin titanium foils are porous to the helium gas present in the channel. Consequently, the electron-gun vacuum was poor despite continuous pumping. As a result, arcs developed which punctured the titanium foil. At a foil thickness of 0.0003" the helium diffusion was insignificant and the E-gun could be operated up to a potential of 50 kV, above which corona effects became excessive. At 50 kV incident energy, however, few electrons penetrated the 0.0003" foil, such that their effect on the discharge was minimum. What is needed is an electron-gun voltage of twice the above potential which mandates the redesign of the gun for suppression of corona effects.

A photograph of the laser head is presented in Figure 5. The view shows the electron-gun glass envelope and the white Al_2O_3 insultating block which encloses the filament. The filament feedthroughs are visible as they enter an opening in the Al_2O_3 block. The filament itself is near the bottom of the insulating block which rests in a stainless steel plate. The entire electron-gun assembly slides into the teflon shell replacing the aluminum block shown in Figure 3. An exploded view of the entire system is given in Figure 6.

Because of the inadequate performance of the electron-gun, the later laser excitation experiments were conducted with the self-sustained discharge unit shown in Figure 3 employing pulsed excitation.

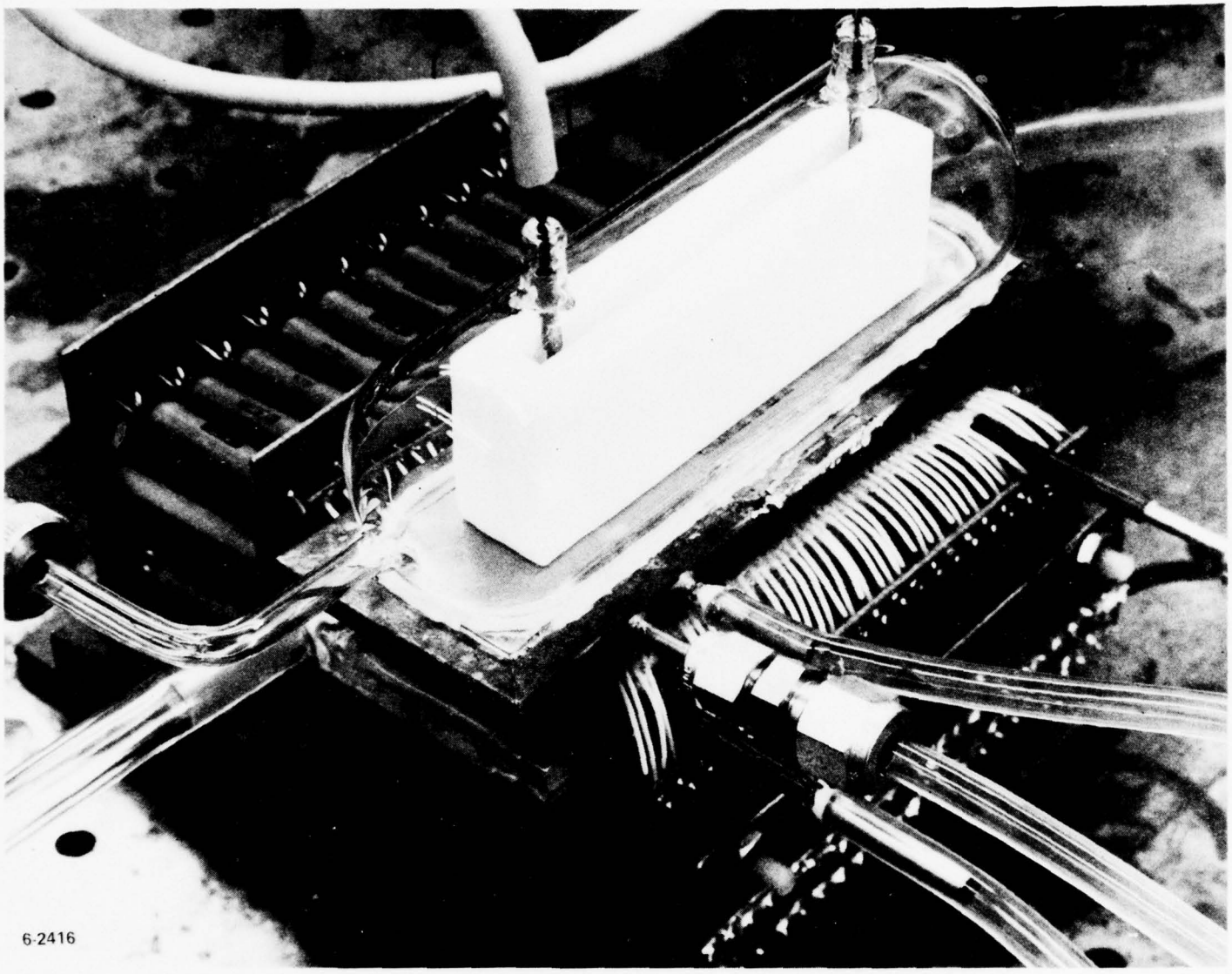

Figure 5. HF Laser Head

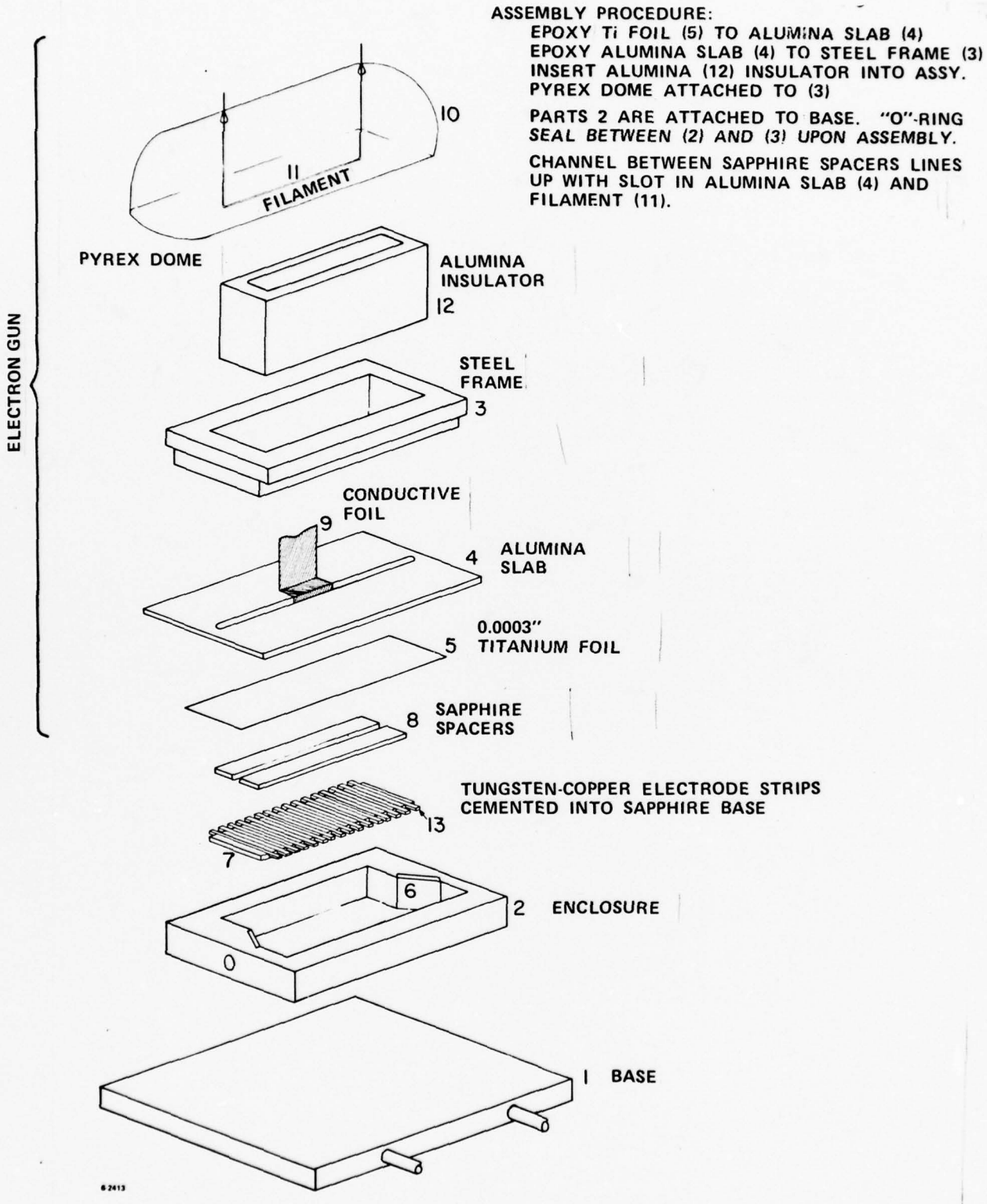

Figure 6. Discharge Vessel-Exploded View.

4.0 EXPERIMENTAL RESULTS

4.1 He/HF SINGLE PULSE DISCHARGES

All 50 capacitors, C_i, of the transversely excited HF waveguide laser were charged through individual resistors, R_i, from a common supply which was also connected to the foil through a choke serving to stabilize the discharge. Upon a trigger command, a hydrogen thyratron provided a conduction path to ground causing the capacitor voltage to appear across the discharge gap (see Figure 2). The discharge was operated at pulse rates between 1 to 100 pps and the applied voltage was varied from a threshold value of 0.5 to a maximum value of 3.0 kV. At the higher potentials the gap array was substantially over-volted such that rapid breakdown occurred upon thyratron ignition. The partial pressure of HF and He were varied between 1 to 10 torr, and 150 to 500 torr, respectively.

Conventionally, the first step in the study of laser excitation involves the observation of fluorescence emitted by the active medium. At the threshold of level inversion the fluorescence exhibits a nonlinear increase in intensity and a narrowing of its spectrum. But even below that threshold the intensity of the flourescent radiation gives a good indication of the relative population densities in the upper and lower laser levels.

A portion of the radiation which emerged from the active medium (discharge plasma) was focused onto a cooled InSb photodetector. A narrow interference filter was placed in front of the photodetector to separate the HF fluorescence from the broadband infrared background emitted by the plasma.

An oscillograph trace of the photodetector outputs vs time is shown in Figure 7-A for the case of a pure He-discharge at 275 torr. The unexpected occurrence of infrared fluorescence radiation from an He-discharge was baffling at first considering that the lowest excitation potential for He is 19.25 V. But it was subsequently discovered that this radiation is associated with residual water vapor, a contamination coming from the HF bottle. The photodetector output for a He/HF mixture is presented in Figure 7-B. Here, the discharge current is less than one half the helium discharge current even though the applied voltage was the same in both cases. As a result of this drop in discharge current (see Appendix D) the water vapor emission was sharply reduced. On the scale of Figure 7-B the peak of the water vapor background fluorescence corresponds to a relative intensity of less than 8 mV. The photodetector pulse shown in Figure 7-B therefore is mainly due to the HF fluorescence. This is confirmed by the slower pulse decay - when compared to Figure 7-A because of the relatively long radiation time constant of HF(1). The measured decay time of 3.2 μsec for HF(1) is in reasonable agreement with published rate constants (Reference 10).

The amplitude of the fluorescence pulse in Figure 7-B is proportional to the instantaneous number of excited HF molecules. Calculations (see Appendix E) indicated that the peak value of 25 mV for the pulse displayed in Figure 7-B corresponds to a relative population of $N_1/N_0 = 0.15$ which is equivalent to a vibrational temperature of 3150°C (see equation A-5 in Appendix A). Even for

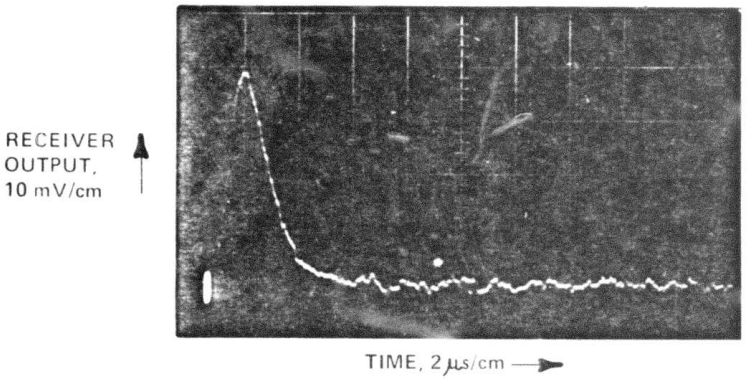

A. PHOTO SIGNAL · 275 Torr He ONLY

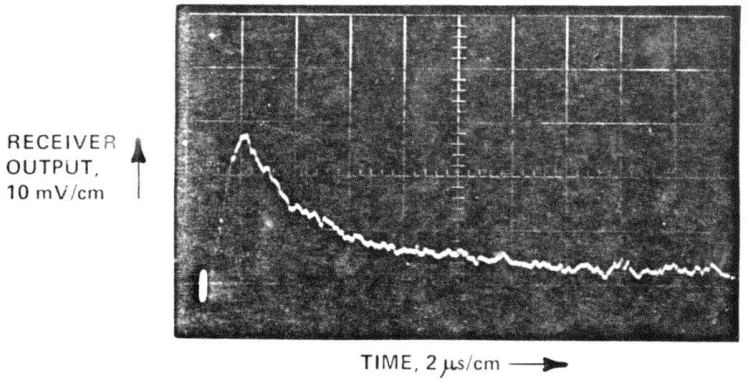

B. PHOTO SIGNAL · 275 Torr He + 5 Torr HF

Figure 7. Fluorescence Pulses for He and He/HF Single Pulse Discharges.

small N_1/N_0 values there are P-branch transitions with optical gain according to equation (1). But their J-numbers are the higher the lower the vibrational temperature according to equation (1) and the rotational population distribution decreases rapidly with J-number (see Appendix A) as

$$N_r = N_1 \frac{hcB}{kT_r} (2J+1)\, e^{-\frac{hc}{kT_r} B\, J\, (J+1)} \qquad (4)$$

where: h = Planck's constant

c = velocity of light

k = Boltzmann's constant

As a consequence, the gain for high J-number transitions is extremely small and its effect is negated by the scattering loss.

To calculate the gain factor associated with the increased N_1/N_0 ratio the rotational temperature must be known. The nearly instantaneous equilibrium of the rotational motion of HF with the kinetic motion of the buffer gas justifies the assumption $T_r = T = 300^{\circ}K$ (see Appendix A).

The formula for the exponential gain factor (derived in Appendix A) is given by

$$g_o = \frac{hc}{kT_r} B\, (2J+1) \left\{ N_1\, e^{-\frac{hc}{kT_r} BJ\, (J-1)} - N_0\, e^{-\frac{hc}{kT_r} BJ(J+1)} \right\} \frac{\lambda^2 A}{8\pi\Delta\nu} \qquad (5)$$

where: λ = optical wavelength

A = Einstein coefficient for HF(1) = 10^2 sec^{-1} (Ref. 14)

$\Delta\nu$ = linewidth = 350 MHz (Ref. 3)

It can be shown that for 5 torr partial HF pressure, $T_r = 300^{\circ}K$ and $T_v = 3150^{\circ}K$ the maximum gain (attained on $P_1(10)$) is only g_o = 0.0003/cm which is certainly masked by scattering losses.

However, it is very encouraging that the gain grows rapidly with further increases in vibrational temperature. For instance, at $T_v = 4950^{\circ}K$ ($N_1/N_0 = 0.3$) the inversion peak is shifted to $P_1(7)$ with an exponential gain factor of 0.14 cm. The one-way gain along the 8 cm plasma length would exceed 300 percent. The increase in discharge current necessary to bring the population ratio from its present level of $N_1/N_0 = 0.15$ to a value 0.30 is more than double its present value since additional relaxation reactions will become effective.

The peak current densities measured for the present device under the specified operating conditions was 0.5 a/cm^2 corresponding to an electron density of $\approx 1 \times 10^{12}$ cm^{-3} (see Appendix D).

What limits the current density in the present device is the loss of electron energy by inelastic collision with the HF molecules, electron attachment to HF and the electron emission mechanism at the cathode surface. The charge voltage applied throughout these experiments was optimized near 2000 V. Only a fraction of that voltage appears across the gap, the difference is consumed in reactive circuit elements. Further increases in gap voltage did not lead to an increase in fluorescence intensity, probably because the higher drift field enhances the number density of energetic electrons for which the probability of HF(1) excitation is small.

The basic inefficiency here is that the electric field necessary to strike a glow discharge in the He/HF mixture is much higher than the optimum field for efficient vibrational excitation

of HF. Preionization-excitation schemes can be used to overcome this problem (References 15 and 16). Working with a transversely excited CO_2 waveguide laser similar in construction to the here discussed discharge vessel, Wood, et al (Reference 17) have developed a technique whereby a high degree of preionization is achieved through the application of a 20-nsec duration high-voltage pulse followed by a second pulse providing low-voltage dc of opposite polarity. The high degree of ionization was achieved by a combination of secondary emission from the oxidized cathode (Malter effect, Reference 18) and electron multiplication due to the high electric field. Unfortunately there was not sufficient time under this program to implement this modification.

4.2 $He/H_2/HF$ DOUBLE PULSE DISCHARGES

In an attempt to increase the HF excitation rate by exploiting the vibrational excitation transfer from H_2 to HF, double-pulse discharges were generated for a gas mixture of He, H_2 and HF, the two pulses being separated by several μsec. A discharge circuit schematic is shown in Figure 8-B and the monitored cathode potential as a function of time is represented by an oscillograph trace (Figure 8-A). The cathode potential was measured relative to ground. The first pulse is generated when the 0.02 μf capacitor on the primary side of the transformer is discharged through the thyratron. After this initial pulse the cathode potential drops steadily towards more negative values until the voltage across the discharge gaps reaches a breakdown value and the second discharge pulse is formed.

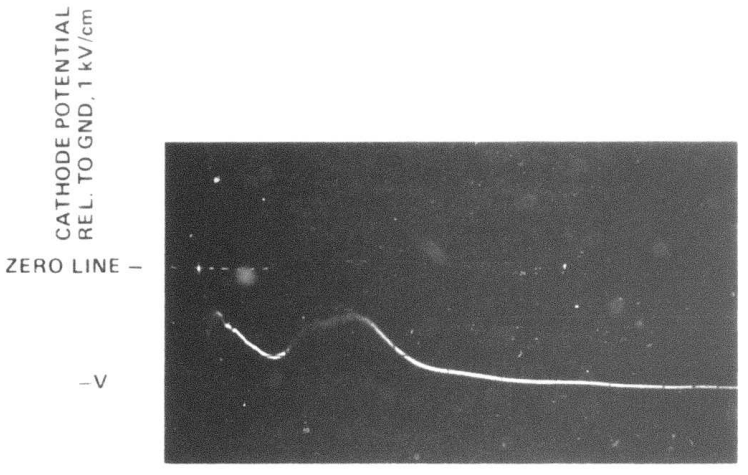

A. CATHODE POTENTIAL vs TIME FOR DOUBLE PULSE DISCHARGE

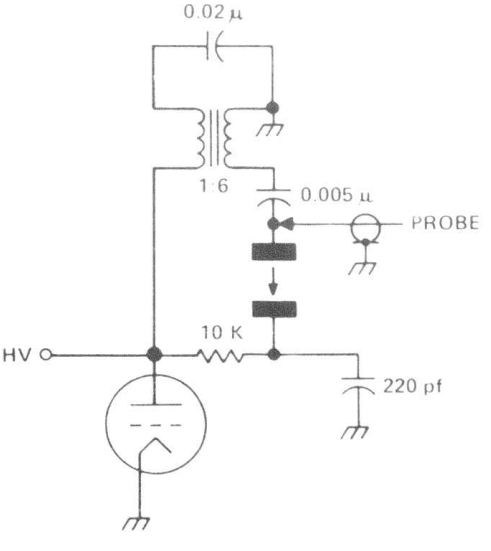

B. DISCHARGE CIRCUIT

Figure 8. Double Pulse Discharge.

This experiment yielded a particularly illustrative demonstration of the H_2 to HF excitation transfer process as shown in a series of oscilloscope traces displayed in Figure 9. These traces represent photodetector outputs as a function of time. Trace A is for a discharge in 283 torr He. The observed infrared fluorescence is the above cited water vapor emission centerd at $\lambda = 2.7$ μm. Trace B shows that the water vapor emission is reduced to the receiver noise level when 1.5 percent H_2 is added to the helium. The reason for this is a reduction in discharge currents due to the loss mechanisms discussed in Appendix D.

When 1.4 percent HF is added to the mixture, the occurrence of its characteristic fluorescence (trace C) can be observed. On this scale the water vapor emission background is less than 2 mV. The sequence of traces D, E and F illustrates the H_2 to HF excitation transfer. In all three cases the partial pressures for He and HF are 283 and 10 torr, respectively. The partial pressure of H_2 is varied from zero (trace D) to 5 torr, (trace E) and 17 torr, (trace F). Note, how the peak amplitude of the second pulse increases relative to that of the first with increasing H_2 concentration. This phenomenon is interpreted as delayed H_2 to HF excitation transfer. The transfer which occurs with a reaction time constant lower than the width of the first pulse is not fully effective during the first pulse. In fact the height of the first pulse decreases with H_2 concentration, again because of the familiar reduction in discharge current as discussed in Appendix D. On the second pulse however, the H_2 to HF excitation transfer becomes effective

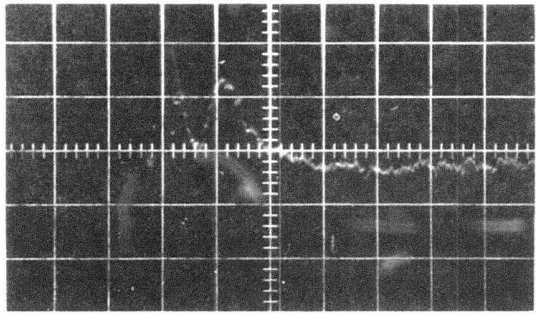

283 He

A

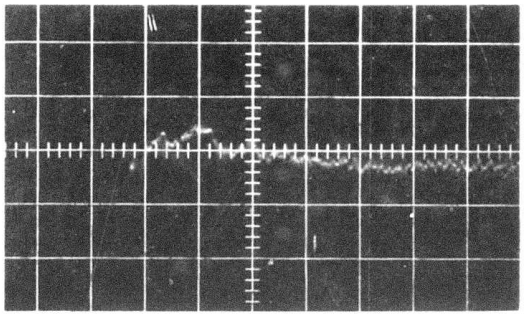

283 He/4 H_2

B

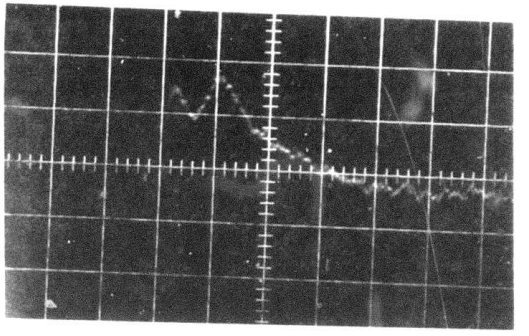

283 He/5 H_2/4 HF

C

D

283 He/10 HF

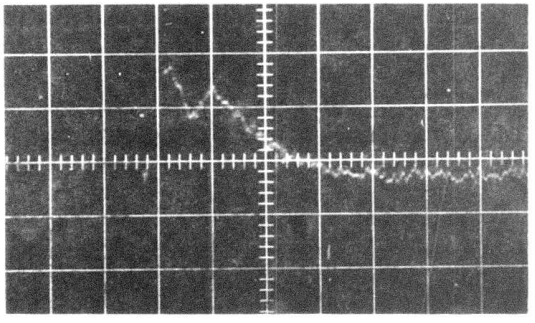

E

283 He/5 H_2/10 HF

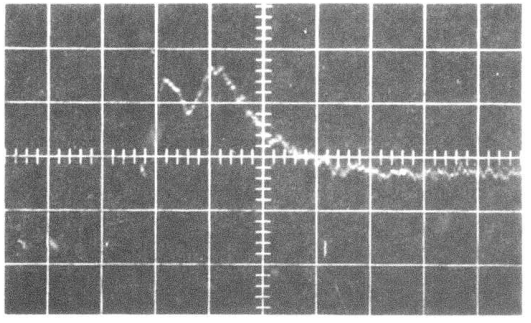

F

283 He/17 H_2/10 HF

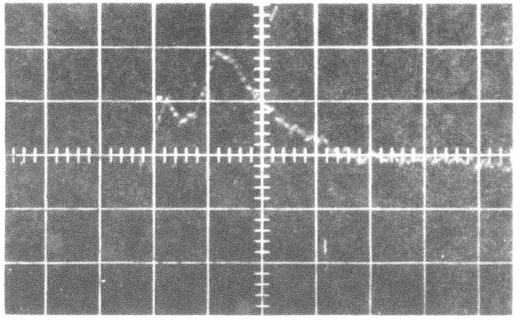

ALL TRACES

HORIZ SCALE: TIME, 5 μs/cm

VERT SCALE: RECEIVER OUTPUT, 10 mV/cm

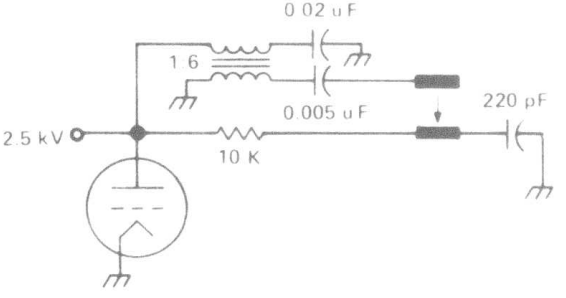

Figure 9. Double Pulse Fluorescence Data.

yielding a relative increase in pulse height with H_2 concentration. The ratio of the second to the first pulse goes from 7/10 for no H_2 to 9/8 at 5 torr H_2 and 10/5 at 17 torr H_2. To a first approximation one may conclude that for the last case (trace F), the pumping rate via H_2 to HF transfer is at least twice that of direct electron collisional HF excitation. In absolute numbers the improvement in HF excitation is only by a factor 10/7. While the H_2 increases the HF excitation rate, it also lowers the discharge current by the previously cited loss mechanism. As a consequence, the observed HF fluorescence intensity indicates that the $He/H_2/HF$ -discharge did not provide a higher vibrational temperature than was obtained for the He/HF discharge. But it is worth noting that a relatively high HF concentration could be tolerated. This offers the possibility of higher saturation densities and wider spectral bandwidth for the active transition; i.e., more potential laser power and tunability.

5.0 SUMMARY

The aim of this program was to investigate the feasibility of purely electrical HF lasers where HF molecules, heavily diluted in a buffer gas of near atmospheric pressures, are vibrationally excited by collisions with free electrons in a discharge plasma confined to a rectangular capillary of 1 x 1 mm cross-section and 8 cm length.

There are substantial difficulties in generating the required electron densities of more than 10^{12} cm^{-3} in the gas mixture of interest while simultaneously maintaining a low gas temperature. Electron attachment to HF tended to reduce the plasma conductivity.

A high discharge field must therefore be applied, much larger than the optimum field for efficient vibrational excitation of HF. Consequently, there is excess gas heating which may frustrate the lasing mechanism. To overcome this problem two special excitation methods were investigated:

- Pulsed discharges, where the thermal energy for one pulse is too small to increase the gas temperature significantly, and
- Electron beam augmentation, where the charge carriers are produced by injected high energy electrons, and the secondary electrons are driven by a small field adjusted for optimum vibrational excitation.

The principle of partial inversion makes use of the difference in relaxation rates for HF rotational and vibrational motion which results in a high vibrational and a low rotational temperature and yields population inversion for certain P-transitions.

By applying $\sim$1 μsec electrical pulses to a gas mixture of 5 torr HF and 275 Torr He, peak electron densities of $\sim 1 \times 10^{12}$ cm^{-3}, and vibrational temperatures in excess of $3000^{o}K$ were achieved while the rotational temperature was near ambient. These values suggest that the $P_1(10)$ transition and those of higher rotational quantum number were inverted. But the relative population in those levels is extremely small and the optical gain apparently blanketed by scattering losses. This result is nevertheless encouraging in that such a simple TE-discharge brought the plasma within reach of a lasing condition.

The measurements indicated that it was the cathode emission which limited the discharge current. A modification of the present device is suggested, involving the Malter effect to enhance cathodic emission to the level required for laser action.

The major problem in obtaining CW operation is the construction of an appropriate electron-gun and its integration into the discharge apparatus. The original goal was to limit the acceleration potential to 50 keV by employing a 0.0001" thin titanium electron-beam window. Several electron-guns of this design were built and tested but it was found that helium diffused from the discharge vessel through the foil into the electron-gun and that the foil thickness had to be increased to 0.0003" to eliminate this problem. However, only a few of the incident 50 keV electrons penetrate the thicker foil. It is therefore suggested that the electron-gun be redesigned for 100 keV or that a plasma cathode be substituted for the thermionic one, since the former operates in a helium gas and therefore may tolerate a certain rate of He leakage by the E-gun window.

A further result of this program was the demonstration of a delayed H_2 to HF excitation transfer. Electrical double-pulses of 5 μsec separation were applied to a $HF/H_2/He$ gas mixture. The H_2 molecules stored vibrational energy gained in the first pulse and released it during the second one. This phenomenon could be employed to stretch HF laser pulses and may be of interest for HEL studies.

REFERENCES

1. J.J. Hinchen and R.J. Freiberg, Appl. Optics 15, pp 459-461, Feb. 1976.
2. "Ladar Device Characterization," Final Report on Contract DASG60-75-C-0046 by TRW, Nov. 1976.
3. S.R. Byron, et al, Final Report on N00014-72-C-0430 and Appl. Phys. Letter 23, pp 565-567, 15 Nov. 1973.
4. R.M. Osgood and D.L. Mooney, Appl. Phys. Lett. 26, pp 201-204, 15 Feb. 1975.
5. G.E. Caledonia and R.F. Center, J. of Chem. Phys. 55, pp 552-561, 15 July 1971.
6. C.E. Treanor, et al, J. of Chem. Phys. 48, pp 1798-1807, 15 Feb. 1968.
7. J.C. Polany, Appl. Optics Suppl. on Chemical Lasers, pp 109-127, 1965.
8. M.A. Kovacs and M.E. Mack, Appl. Phys. Lett. 20, 487, 1972.
9. J.F. Bott and N. Cohen, J. of Chem. Phys. 58, 4549, 15 May 1973.
10. J.J. Hinchen and R.H. Hobbs, J. of Chem. Phys. 65, pp 2732-2739, 1 October 1976.
11. P.M. Smith, et al, Optics Communications 16, 50, Jan. 1976.
12. A. Stein, IEEE J. of Quant. Elect. QE10, 427, April 1974.
13. J.J. Degnan and D.R. Hall, IEEE of Quantum Electronics QE-9, pp 901-910, Sept. 1973.
14. J.K. Hancock and W.H. Green, J. of Chem. Phys. 57, pp 4515-4529, 1 Dec. 1972.

15. J.P. Reilly, J. Appl. Phys. 43, 3411 (1972).

16. A.E. Hill, Appl. Phys. Lett. 22, 670 (1973).

17. D.R. Wood, P.W. Smith, C.R. Adams and P.J. Maloney, Appl. Phys. Lett. 27, pp 539-541, 15 Nov. 1975.

18. E. Nasser, "Fundamentals of Gaseous Ionization and Plasma Electronics," Wiley, 1971.

19. A. Yariv, "Quantum Electronics," Wiley, N.Y. 1967, p 237.

20. G. Herzberg, "Molecular Spectra and Molecular Structure," Vol. I, Van Nostrand, Princeton.

21. A.V. Engel, "Ionized Gases," Oxford Press, 1965.

22. A.S. Denholm, Energy Sciences, Private Communications

APPENDIX A

PARTIAL INVERSION CRITERION AND LASER GAIN

The general expression for laser gain is given (Ref. 19) as:

$$g_o = \left(N_{1,J-1} - N_{0,J}\frac{g_{J-1}}{g_J}\right)\frac{\lambda^2 A}{8\pi\Delta\nu}\sqrt{\frac{4\ell n2}{\pi}} \qquad \text{(A-1)}$$

$N_{1,J-1}$, $N_{0,J}$ = population densities for the upper (1,J-1) and lower (0,J) laser level, respectively

g_{J-1}, g_J = degeneracies for the respective levels, $g_J = 2J+1$

λ = laser wavelength = 2.7 - 2.9 μm

A = Einstein coefficient for the laser transition = 10^2 sec^{-1} (Ref. 14)

$\Delta\nu$ = spectral half width of the transition = 350 MHz (Ref. 3)

The population distribution over the rotational sub-levels for the lower vibrational state is given (Reference 20) by

$$N_{0J} = N_0 \frac{hcB}{kT_r}(2J+1)\, e^{-\frac{hcB}{kT_r}J(J+1)} \qquad \text{(A-2)}$$

A similar term can be written for $N_{1,J-1}$.

N_0 = total population density of the v = 0 state (summed over all rotational sub-levels)

B = rotational energy constant for HF = 20.9 cm^{-1}

T_r = rotational temperature

J = rotational quantum number

h,c,k = familiar natural constants

From equations (A-1) (A-2), it follows that

$$g_o = \frac{hcB}{kT_r}(2J+1)\left(N_1 e^{-\frac{hcB}{kT_r}J(J-1)} - N_0 e^{-\frac{hcB}{kT_r}J(J+1)}\right)\frac{\lambda^2 A}{8\pi\Delta\nu}\left(\frac{4\ell n2}{\pi}\right)^{1/2} \quad (3)$$

Equation (A-1) yields the threshold condition

$$N_{1,J-1} \geq N_{0,J}\ \frac{g_{J-1}}{g_J} \quad (A-4)$$

It is customary to associate the ratio of population densities between two vibrational levels (here v = 1 and v = 0) with a vibrational temperature T_v defined by the Boltzmann equation

$$\frac{N_1}{N_0} = e^{-\frac{hc\omega_e}{kT_v}} \quad (A-5)$$

where ω_e is the vibrational energy constant.
Using the above equations one may write the threshold condition in the form

$$2J\ \frac{B}{T_r} \geq \frac{\omega_e}{T_v} \quad (A-6)$$

Let us consider the example $\frac{N_1}{N_0} = 3$, $T_r = 300^oK$, $N_1+N_0 = 1.77\ 10^{17}\ cm^3$ (5 torr HF). The maximum gain is attained for J = 7, $g_o = 0.14/cm$.

For CW operation the optical power inside the resonator can be estimated from the expression

$$P_i = x^2\ S\ g_o\ \ell \quad (A-7)$$

$$S = \frac{h\nu}{\sigma_{opt}}\ \gamma \quad (A-8)$$

x = width and height of rectangular plasma channel,
= 0.1 cm

ℓ = length of plasma channel = 8 cm

S = saturation intensity

$h\nu$ = quantum energy $\sim 7\ 10^{-20}$ W sec

σ_{opt} = cross-section for stimulated emission

γ = decay rate of the upper laser level (collisional deactivation) = $3.8\ 10^{5}$ sec^{-1} at 5 torr HF

The cross-section for stimulated emission, $\sigma_{opt} = \frac{\lambda^2 A}{8\pi\Delta\nu} \left(\frac{4\ell n2}{\pi}\right)^{1/2}$ was used above and is equal to $\sigma_{opt} \sim 1 \times 10^{-15}$ cm^2. Substituting the above values into equations (A-7) and (A-8) yields $S = 24$ W cm^{-2}, and $P_i = 270$ mW, of which about half can be extracted from the cavity. For pulsed discharges the stored optical energy is given by

$$E_S = \frac{1}{2} h\nu\ N_1\ x^2 \cdot \xi \cdot \ell \qquad \text{(A-9)}$$

where ξ is a coefficient defining the degree of cross-coupling between rotational states.

For the above example $N_1 \sim 3.5 \times 10^{16}$ cm; assuming $\xi = 0.1$ we find $E_S \approx 10$ μJ. One of the advantages of a capillary TEA laser is that it lends itself to high repetition rate operation since the time periods for pulse formation are extremely short, ≈ 10 nsec. Pulse rates of 10^4 - 10^5 pps appear feasible (Reference 11).

Pulsed excitation leads to a step function rise in gas temperature since the rotational energy (activated by electron collisions) is instantaneously converted into kinetic energy of the buffer gas atoms. The temperature rise is given by

$$\Delta T = \frac{i_o X_o \; x \; \tau \; C_r}{V \; N_{He} \; \frac{3}{2} \; k} \qquad \text{(A-10)}$$

i_o = peak discharge current = 0.3 a

X_o = peak drift field = 5500 V

x = gap width = 0.1 cm

τ = pulse width = 0.8 μsec

C_r = fraction of discharge energy coupled into rotational motion of HF = 0.05

V = plamsa volume = 0.08 cm^3

N_{He} = number of He atoms per cm^3 ($\sim 10^{19}$ cm^{-3} at 283 torr partial pressure)

k = Boltzmann constant

Inserting these parameters into equation (A-10) yields a temperature rise of $\Delta T \sim 0.4^{o}C$. For repetitive pulsing the temperature will rise until an equilibrium is established by thermal conduction to the capillary walls.

APPENDIX B

EXCITATION TRANSFER H_2 TO HF

For discharges in mixtures of He, H_2 and HF gas the excitation of HF to its first vibrational level occurs in two ways: by direct electron impact and indirectly via H_2 to HF excitation transfer. The H_2 molecules themselves are excited by electron impact. The transfer reaction

$$H_2(1) + HF(0) \underset{k^-}{\overset{k^+}{\rightleftharpoons}} H_1(0) + HF(1) + \Delta E \ (200 \ cm^{-1} \ hc) \qquad (B\text{-}1)$$

occurs with different rates in both directions, whereby the forward to backward reaction rates relate as

$$k^+ = k^- \ e^{+\Delta E/kT} \qquad (B\text{-}2)$$

where T is the kinetic gas temperature. The population density in the HF(1) state is governed by the following equilibrium rate equation:

$$k^+ \ M_1 N_0 = k^- \ M_0 N_1 + k_1 \ N_1 N_0 \qquad (B\text{-}3)$$

k_1 = rate constant for HF collisional self-quenching

N_0, N_1 = population densities in ground and first excited levels of HF, respectively

M_0, M_1 = population density in ground and first excited level of H_2, respectively

From equations (B-1), (B-2), and (B-3), it follows that

$$\frac{N_1}{N_0} = \frac{M_1}{M_0} \frac{e^{\Delta E/kT}}{1 + \frac{k_1 N_0}{k^- M_0}} \qquad (B\text{-}4)$$

At room temperature $k_1 = 6 \times 10^4$ sec^{-1} torr^{-1} (Reference 10) and $k^- = 1.7\ 10^4$ sec^{-1} torr^{-1} (Reference 9). If the H_2 concentration is ten times that of HF, equation (B-4) yields the relation

$$\frac{N_1}{N_0} \sim 2 \quad \frac{M_1}{M_0} \qquad (B\text{-}5)$$

i.e., the population ratio for the v = 1 and v = 0 states of HF is twice that for H_2. The relative excitation of H_2 itself, $\frac{M_1}{M_0}$ is determined by the equilibrium between collisional excitation and relaxation of the $H_2(1)$ state.

APPENDIX C

ELECTRON TRANSMISSION THROUGH AN E-GUN WINDOW

Data on electron transmission through thin foils were not available at the energy ranges of interest. Therefore, the available data was scaled and extrapolated as follows. From Figure C-1A (Reference 22) one ascertains that a 0.0005" titanium foil transmits about 87 percent of the electrons at an incident energy of 150 keV. By extrapolation of the measured electron ranges in air (Figure C-1B) it is estimated that the range drops from 32 mg/cm^2 at 150 keV incident energy to 6 mg/cm^2 at 50 keV. Assuming that this ratio also holds for metals, the foil thickness must be scaled by 6/32 in order to obtain an electron transmission of 87 percent at 50 keV: i.e., the titanium foil thickness must be 0.0001".

During the course of this investigation it was observed that such extremely thin titanium foils were porous to helium gas which diffused from the active channel through the foil into the electron-gun plenum and compromised the vacuum. As a result the E-gun developed arcs which punctured the foil.

However, 0.0003" foils were found to work excellently, even at repetition rates of up to 100 pps. Once the foil was properly attached to the backing structure the vessel was operated one to two hours per day over several months without any serious foil damage. Unfortunately, at a maximum "safe" electron-gun voltage of 50 keV the transmission through a 0.0003" foil was extremely small and the injected electron beam had only a marginal effect on the plasma.

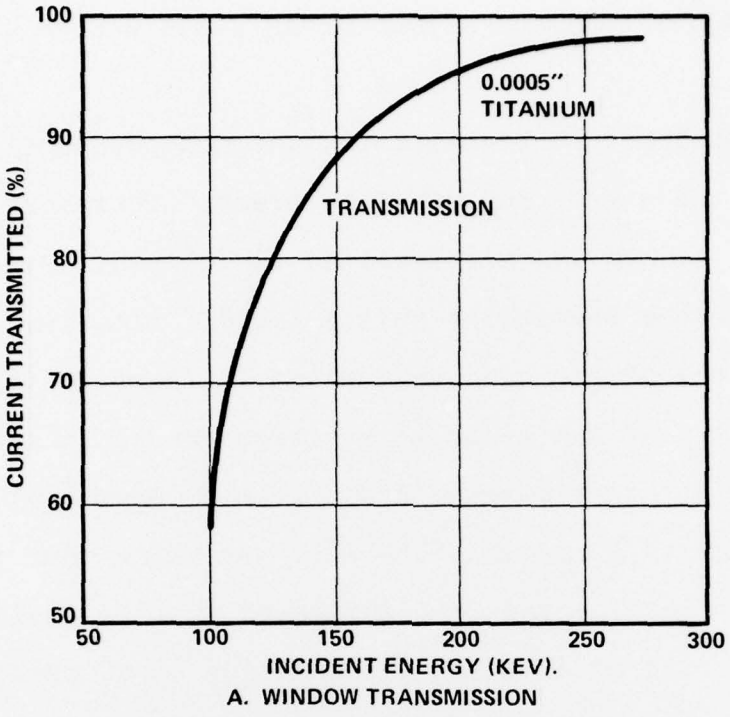

A. WINDOW TRANSMISSION

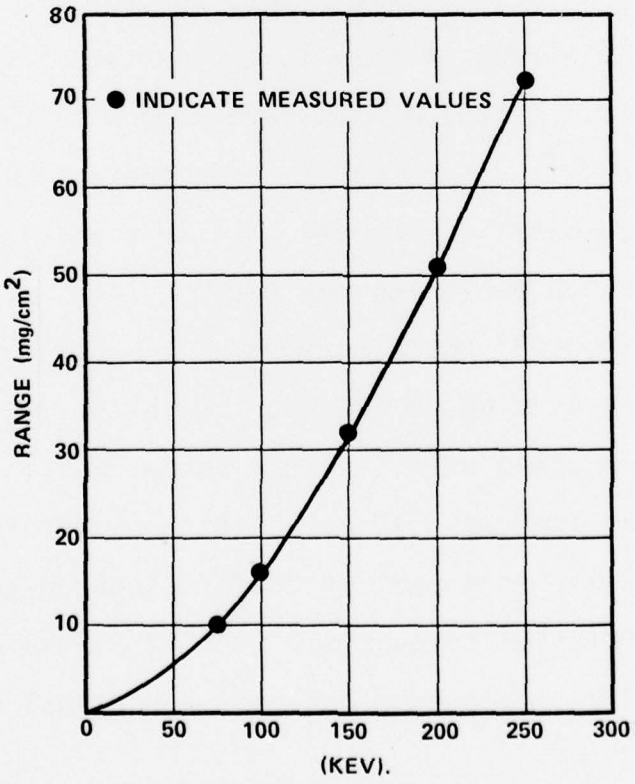

B. ELECTRON RANGE AIR AT NTP

Figure C-1. Electron Transmission in Titanium Foils and Air.
(Data from Energy Sciences Inc.)

APPENDIX D

DISCHARGE CURRENT CALCULATIONS

In a pure He-discharge the free electrons lose their kinetic energy predominantly by elastic collisions where the average fractional loss is small. Very few collisions are inelastic since the lowest excitation potential in He is 19.75 eV. Although infrequent, inelastic collisions are crucial to the maintenance of the discharge since some of them lead to the ionization of He atoms (at 24.5 eV) to produce the charge carriers.

CW discharges exhibit a voltage-current characteristic which is determined by an equilibrium between ionization and recombination. "Overvolting" a discharge; i.e., applying an electric field in excess of the equilibrium value leads to arc formation provided the gas pressure is above a certain minimum value. CW discharges are therefore stabilized by a ballast resistor which effectively limits the voltage across the discharge. Without the ballast the discharge may collapse into an arc shorting out the glow discharge. Arcs develop from local increases in gas temperature - usually near the electrodes - which leads to locally enhanced ionization generating more heat and ionization until a filamentary path of very high current density is established. Where this filamentary current path meets the cathode, the cathode surface is heated until thermionic emission dominates and the cathode fall is eliminated. There are two ways to prevent arc formation: by employing an excitation pulse which is shorter than the arc formation time or by providing adequate thermal diffusion within the gas and the vessel envelope to prevent the formation of local hot spots.

For the here described HF/He discharges, the capillary geometry provided a short thermal conduction path; good turbulent mixing in the capillary was ensured by flowing the gas through the capillary. It is not clear however whether the duration of the excitation pulse was less than the arc formation time which may be rather short in such a narrow gap discharge. The suppression of arcs becomes particularly difficult when increasing pressures, p, since the thermal dissipation in the cathode fall increases with p^3 (Reference 21).

The discharges in the capillary vessel discussed here remained stable even when the pressure was turned up to atmospheric values and the gaps overvolted to several times the breakdown value.

The striking difference between noble gas and molecular discharges was observed when small amounts of HF or H_2 were added to a helium discharge plasma. A molecular portion of less than two percent caused current reductions of up to a factor of 5. In the case of HF, the effect can in part be accounted for by electron attachment but for H_2, inelastic collisions are responsible for the drastic reduction in discharge current. Due to the difference in mass the fractional loss for elastic collisions with He is only 5×10^{-3}. Hydrogen molecules on the other hand exhibit a great number of quantum levels throughout the energy spectrum of the free electrons in the plasma. The fractional losses for electrons by inelastic collisions with molecules are of course equal to the quantum energy of the interacting molecular state; i.e., they are large. Consequently, the electron losses increase with the addition of the

molecular species. For an estimated $\frac{X}{p}$ value of 20 $\frac{V}{cm}$ torr (X = electric drift field in positive column) the loss factor for discharge electrons is $\kappa = 5 \times 10^{-3}$ for He and $\hat{\kappa} \approx 0.1$ for H_2 (Reference 21). The effective loss factor for 1.0 percent H_2 in He is thus $\kappa' = 1.2\ \kappa$. The primed values relate to the H_2-doped discharge whereas the unprimed parameters are associated with the pure He-discharge.

The electron temperature in the plasma is related to the $\frac{X}{p}$ value and loss parameter κ via the formula (Reference 21)

$$\frac{X}{p} = T_e \sqrt{\frac{2\kappa}{\lambda_1}} \qquad \text{(D-1)}$$

where λ_1 is the mean free path for electrons at 1 torr gas pressure. With $\lambda_1 = 0.04\ cm^{-1}$ at $\frac{X}{p} = 20\ \frac{V}{cm}\ torr^{-1}$ He (Reference 21) one gets from equation (D-1) for a pure He discharge $T_e \hat{\approx} 8$ eV; (i.e., $\frac{3}{2} kT_e = 8$ eV). For a 100:1 He/H_2 mix the electron temperature is (according to D-1) reduced to $T_e' \hat{\approx} T_e/1.1$. The ionization rate scales as

$$\frac{Z'}{Z} = \sqrt{\frac{T_e'}{T_e}} \cdot \frac{e^{-\frac{eV_i}{kT_e}}}{e^{-\frac{eV_i}{kT_e}}} \qquad \text{(D-2)}$$

V_i = ionization potential

e = elementary charge constant

k = Boltzmann's constant

Inserting $V_i = 24.5$ eV and the above parameter values into equation (D-3) yields $Z' = 0.57\ Z$.

This reduction in charge carrier generation is reflected in a decrease in discharge current as illustrated in Figure D-1A where the output of an inductive pick-up circuit is displayed against time. (The curves are redrawn from oscillograph traces.) The current is monitored at the secondary winding of a torroidial transformer whose primary winding carries the discharge current.

Traces No. 1 and 2 in Figure D-1A correspond to a discharge in pure He and a 100:1 He/H_2 mixture, respectively. The pulse amplitude is proportional to the induced voltage:

$$V = aL_{12}\, di/dt \qquad (D\text{-}3)$$

where L_{12} is the mutual inductance of the transformer, and @ an attenuation constant.

The traces in Figure D-1A have a large negative component which is associated with the rapid current build-up upon thyratron ignition. The here displayed positive part of the pick-up voltage approximates the exponential decay profile of an RC circuit (the draining of the discharge capacitors through the plasma):

$$V = V_o\, e^{-t/\tau} \qquad (D\text{-}4)$$

According to equations (D-3) and (D-4) the relation between peak current, peak voltage and decay time constant for the traces in Figure D-1A relate as

$$V_o = aL_{12}\, i_o/\tau \qquad (D\text{-}5)$$

Note, that the discharge circuit for the single pulse discharge (Figure D-1B) is quite different from the double pulse circuit described in Section 4.2. Both types of discharges were employed, the former generally for He/HF mixtures, and the latter for $He/H_2/HF$ gas mixes.

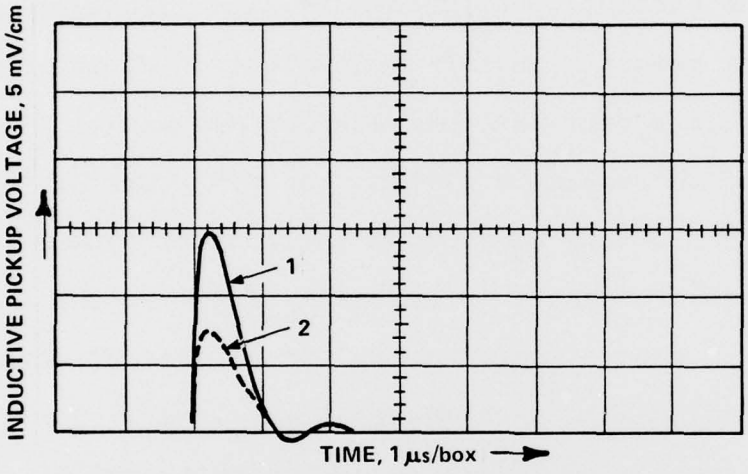

A. SIGNAL ON TOROID SECONDARY AFTES 20 dB ATTENUATION.

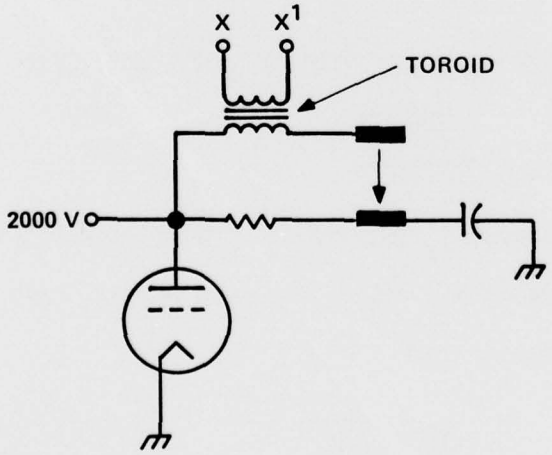

B. DISCHARGE AND MONITOR CIRCUIT.

Figure D-1. Single Pulse Discharge Current Data.

By a calibration measurement it was determined that $(a \cdot)(L_{12}) = 1.9\ 10^{-8}$. From trace No. 1, Figure D-1A one reads the values V_o = 15 mV and τ = 0.8 μsec which (according to equation D-5) yields the peak current value of i_o = 0.63 a. For a total anode surface area of = 0.5 cm^2, the current density then is j_D = 1.26 a/cm^2. An important current reducing mechanism is electron attachment to HF molecules. This effect has been studied previously (Reference 3). It was found there that addition of 0.35 torr HF to a mixture of 90 torr He/10 torr H_2 reduced the current by ~ 25 percent. The effect is less pronounced in our case, but here the average electron energy is much higher than in the referenced work, and the attachment cross-section correspondingly lower. For the He/HF mix which optimizes the HF fluorescence intensity the discharge current density was 0.5 a/cm^2. The electron density is calculated from the equation (Reference 21)

$$N_e = \frac{j_r^-}{e\ \bar{v}} \qquad \text{(D-6)}$$

where $\bar{v}$ is the average random velocity of the free electrons:

$$\bar{v} = \sqrt{\frac{8kT_e}{\pi m}} \qquad \text{(D-7)}$$

(m = electron mass), and j_r^- is the current density associated with the random electron motion which is related to the drift current density j_D (Reference 21) as

$$\frac{j_r^-}{j_D} = \sqrt{\frac{T_e}{T_i}} \qquad \text{(D-8)}$$

where T_e, T_i are the electron and ion temperatures, respectively. Using the above electron energy of 8 eV ($60,000^{\circ}K$) and an estimated value $T_i = 1000^{\circ}K$ one calculates $j_r^-/j_D = 7.8$. For $j_D = 0.5$ a/cm^2 it then follows that $j_r^- = 3.9$. From equation (D-7) one finds $\overline{v} = 1.5 \times 10^8$ cm/sec and from equation (D-6) $N_e \approx 1 \times 10^{12}$ cm^{-3}.

APPENDIX E

RELATION BETWEEN VIBRATIONAL TEMPERATURE AND FLUORESCENCE INTENSITY

For sufficiently short discharge pulses the excitation of HF molecules is not in equilibrium with the vibrational excitation process and the activation is more or less limited to the first vibrational level. The intensity distribution in the R- and P-branches of the $v = 1 \rightarrow 0$ fluorescence lines is plotted in Figure E-1. During this investigation the fluorescence radiation was measured with an InSb photodetector-amplifier. To discriminate against the radiant emission of residual water vapor (peaked at 2.72 μm) the HF fluorescence was observed in the wings of the P-branch using a narrow spectral filter.

The total fluorescence radiation generated in the plasma was equal to

$$P_{fluorescence} = N_1 \, V \, h\nu \, A \qquad \text{(E-1)}$$

N_1 = population density for HF(1)

V = plasma volume = 0.08 cm^3

$h\nu$ = quantum efficiency = 7×10^{-20} W sec

A = Einstein coefficient for the ($v = 1$) level = 10^2 sec^{-1}

This radiation is locally isotropic , most of it reaching the two ends of the waveguide after one or more reflections at the waveguide walls. Upon emerging from the waveguide the light leaves the vessel on both sides through an opening in the enclosing teflon shell. Each opening defines a numerical aperture of $\alpha = 0.175$.

If the reflections at the waveguide wall were total, half of the fluorescence power would be radiated isotropically at either waveguide end. The fraction of the total fluorescence power leaving through one of the two openings in the teflon wall is equal to

$$\frac{1}{2} = \frac{\alpha^2 \pi/4}{2\pi} = 1.9 \times 10^{-3} \qquad \text{(E-2)}$$

The radiation cone was centered about the waveguide axis and the included rays made small angles with the waveguide axis; i.e., the emerging rays have undergone few reflections in the waveguide with moderate attenuation. An average loss of 0.3 is estimated. The infrared light leaves the vessel through a sapphire Brewster plate, is collimated by an uncoated As_2S_3 lens, then transmitted through a narrowband spectral filter and a sapphire dewar window and focused by a second As_2S_3 lens onto the InSb photodetector. The reflective loss for the Brewster plate is 0.12 (unpolarized light), for the dewar window 0.08 and for the lenses 0.32 each. The above loss factors accumulate to a total loss of 0.73 (0.27 accumulated transmission). Upon evaluating the spectral overlap function of the R- and P-branch fluorescence profiles and the narrowband filter numerically from Figure E-1, an effective transmission of 0.02 is calculated. Multiplying the above transmission values with the term given in equation (E-2), yields that only one part in 10^5 of the HF fluorescence radiation arrives at the focal plane of the second lens where the photodetector is located.

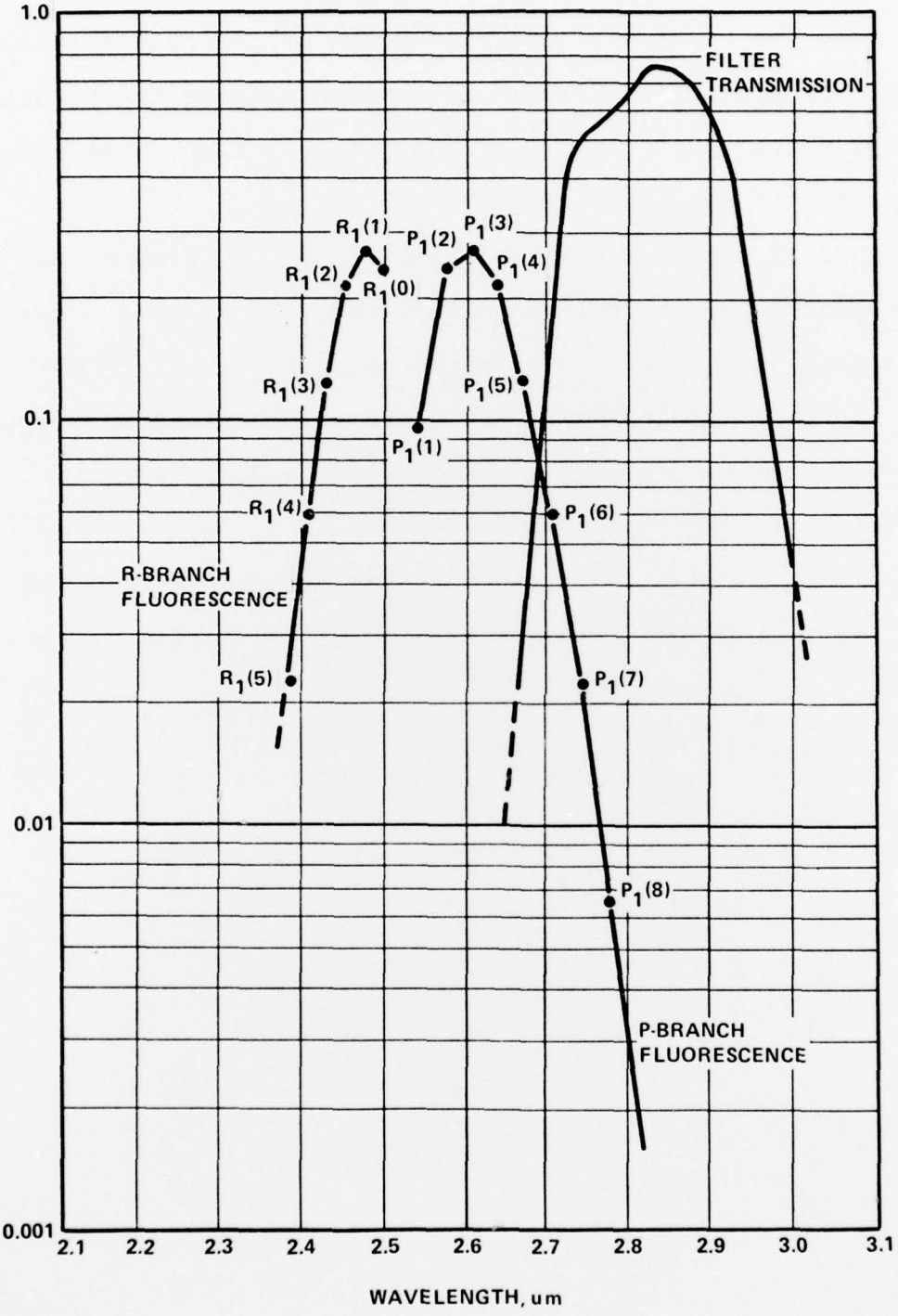

Figure E-1. Spectral Characteristics of HF (1) Fluorscence and Receiver Filter
Ordinate - Relative Population in the Upper Level of R- and P-Transitions, and
Fractional Filter Transmission.

Precise measurements of the focal spot and detector diameters revealed that the focal spot overfilled the active detector area such that only 0.2 of the focused energy impinged on the detector. In summary, a fraction 2×10^{-6} of the total HF fluorescence radiation was received by the detector.

Figure 7B yields a peak receiver output value of 25 mV. Since the overall receiver responsivity was 1 V/μW, this output voltage corresponds to an intercepted power of 2.5×10^{-8} W at the detector surface. According to the above calculations the associated total peak fluorescence power was $\frac{2.5 \times 10^{-8}}{2 \times 10^{-6}} = 0.125$ W which in turn corresponds to an HF(1) population density of $N_1 = 2.2\ 10^{16}$ cm^{-3} according to equation (E-1). Since the HF partial pressure was 5 torr ($N_0+N_1 = 1.77\ 10^{17}$ cm^{-3}) the relative population density was

$$\frac{N_1}{N_0} \approx 0.15 \qquad \text{(E-3)}$$

corresponding to a vibrational temperature of $\approx 3150^{\circ}$K.